International Journal of QUANTUM CHEMISTRY WWW.Q-CHEM.ORG FULL PAPER

Do one-step mechanisms always involve simultaneous evolution of electron density? QTAIM/IQA analysis of the Curtius rearrangement.

José L. López-Fernández,[1] Ricardo A. Mosquera,[2] and Ana M. Graña[3]

Correspondence to: Ana M. Graña (E-mail: *ana@uvigo.es*)

[1] *José L. López-Fernández*
Departamento de Química Física, Facultade de Química, Universidade de Vigo, 36301 Vigo, Galicia, Spain.
[2] *Ricardo A. Mosquera*
Departamento de Química Física, Facultade de Química, Universidade de Vigo, 36301 Vigo, Galicia, Spain.
[3] *Ana M. Graña*
Departamento de Química Física, Facultade de Química, Universidade de Vigo, 36301 Vigo, Galicia, Spain.

ABSTRACT

The Curtius rearrangement reaction is studied by using QTAIM analysis of the electron density and the IQA formalism. Although the rearrangements take place in one stage, two phases are distinguished when the rearranged atom is H: the first one corresponds to the separation of N_2, and the second one to the N-H/C-H bond rearrangement. The transition state (TS) for the reaction does not represent an intermediate between reagent and product for the migration but for the isolation of the N_2 molecule. When the migration is undergone by a fluorine atom no electronic phases can be distinguished and the process is really concerted. As the migration happens closer to the TS, the TS is more similar to the product.
The IQA analysis reveals different electron density evolutions for H and F migrations, and the scarce relevance (in terms of energy) of the point where BCPs appear or disappear.

Introduction

IUPAC Gold Book defines concerted reactions as: "a single step reaction through which reactants are directly transformed into products, i.e. without involvement of any intermediates".[1] No reference is made in this statement about a simultaneous evolution of the set of bonds formed/broken in the process. Nevertheless, concurring evolution of the electron density involved has been widely assumed in chemical literature concerning the mechanism of concerted reactions. As a consequence, in the absence of detailed studies, proposed transition states for concerted mechanisms are generally roughly represented using half formed/broken bonds.

Here we present an example where, for a rigorous concerted processes (it only involves one transition state), different phases could be distinguished. These phases represent clearly different electron density evolutions and affect different atoms and bonds along the reaction. So, the transition state could not be correctly described by half formed bonds.
The example selected is one rearrangement reaction. They are an important group of processes in which an atom or a bond moves from a site in the reagent to a different site in the product. These reactions may occur in a concerted manner or through a step-wise mechanism. In particular, we have studied the Curtius rearrangement shown in Scheme I.[2] The mechanism for this reaction remained unknown

for years. The main point in discussion was if the reaction takes place in one stage or if it occurs in several steps with acylnitrenes (RC(O)N:) as intermediates. Different theoretical studies on aryl and acyl azides show that the syn conformers with respect to the C-N bond are more stable than the anti ones and that for syn conformers Curtius rearrangement occurs in one stage. The barriers for syn/anti isomerization achieve 7-9 kcal mol^{-1} whereas the barriers for the transformation of syn compounds into isocyanates are considerably lower than those for the rearrangement of anti compounds into isocyanates. For this reason the Curtius reaction occurs by a concerted mechanism as shown in Scheme I.

Our objective is to relate the evolution of the energy along the reaction with structural changes in geometries and bond properties and also with atomic properties. For example, we want to analyse the presence of bond critical points (BCP) for the bonds that appear and disappear during the reaction.[3-9] In Quantum Theory of Atoms in Molecules (QTAIM), the existence of a bond path or an atomic interaction line (AIL) is often related to the existence of a chemical bond connecting the atoms.[10,11] However, sometimes no AIL is found where the chemists expect to find a bond. Some other times an AIL is found when a repulsive interaction is assumed between two atoms. There have been many contributions to this debate for years.[12-16]

Recently, the molecular mechanism of the Curtius rearrangement of 3-oxocyclobutane-1-carbonyl azide has been described by using electron localization function (ELF) topological analysis.[17] The authors concluded that the mechanism of the reaction is concerted but asynchronous. In this paper we will try to identify parameters related to the bonds and to the atoms that change during the rearrangement reaction. Specifically, we are interested in how interatomic energies and their contributions vary along these reactions to understand the shape of the corresponding energy profile. For this reason, our study also includes a similar reaction, where fluorine replaces hydrogen as migrating atom. This replacement modifies significantly the energy profile.

The components of the energy were obtained from the Interacting Quantum Atoms (IQA) energy decomposition technique.[18,19] This approach expresses the energy of a molecule as the sum of atomic, E_{intra}, and interatomic, E_{inter}, contributions. We will show that this method is a useful tool to understand the changes along the reaction, which can be satisfactorily employed to establish different phases in a chemical process.

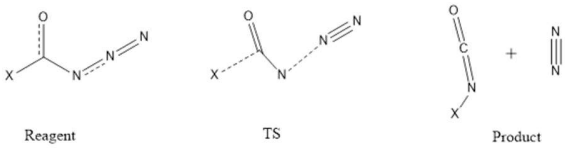

Scheme I

Computational Methods

All calculations were performed by using B3LYP method in Gaussian09 with 6-311++G** basis set.[20] For both reactions intrinsic coordinate (IRC) calculations were carried out. The minima and the transition states were characterized as critical points in frequencies calculations. The wave functions were obtained for reagents, products, transition states and selected points of the path. On these wave functions we performed QTAIM topological electron density analysis by using the AIMAll program to obtain bond and atomic properties and perform IQA analysis to compute interatomic energies and their contributions.[10,11,21]

The value of the electron density at the bond critical points, $\rho(\boldsymbol{r}_c)$, is here employed as an indicator for the existence of a bond. Electron populations, $N(\Omega)$, were calculated by numerical integration of the respective density function. The absolute values achieved for the integrated values of the Laplacian of the electron density in all the atomic fragments, $L(\Omega)$, were smaller than $1.0 \cdot 10^{-3}$ au. The differences between total

electron population and that obtained by summation of properties of the fragments [N-$\Sigma N(\Omega)$], were always smaller (in absolute value) than $2.0 \cdot 10^{-3}$ au.

Delocalization indices (DI) , obtained from overlap integrals of the molecular orbitals, measure the electron population shared by two atoms.[22] The expressions employed for the calculation of DI are strictly valid in the HF approximation and for DFT calculations they are approximations to the corrected DI as, for the KS formalism, the mono-determinant wavefunction is only an approximation to the real one. Moreover, these indices only represent unequivocally the covalent bond order for diatomic molecules and they are invariably somewhat less tan the formal bond multiplicity for polar bonds.[23]

As mentioned above, the components of the energy were obtained from the IQA energy decomposition technique.[18,19] This approach expresses the energy of a molecule as the sum of atomic, E_{intra}, and interatomic, E_{inter}, contributions:

$$E = \sum_{\Omega} E_{intra}(\Omega) + \sum_{\Omega>\Omega'} E_{inter}(\Omega, \Omega') \quad (1)$$

where $E_{intra}(\Omega)$ is the atomic, one-center term corresponding to the net electronic energy of atom Ω. It includes kinetic energy, electron-nucleus potential energy and electron-electron potential energy. The interatomic, two-center terms $E_{inter}(\Omega, \Omega')$ contain various potential energy terms between atoms Ω, and Ω' (V_{nn}, V_{ne}, V_{en} and V_{ee}). The electron-electron term, V_{ee}, can be divided into electrostatic and exchange-correlation contribution. Thus, E_{inter} can be split into two components: $V_{C,}$ an electrostatic term collecting all the classical coulombic energy, and V_{XC} the exchange-correlation term. It is also important to emphasize that the IQA approach is valid for non-equilibrium geometries, whereas the QTAIM atomic energies are only valid for stationary points. The IQA approach can be used for B3LYP functionals as implemented in AIMAll program.[21]

Results and Discussion

Figure 1 shows the energy profile of the Curtius rearrangements for X=H and X=F shown in Scheme I. We first analyze the migration for the hydrogen atom. The reaction evolves from the reagent to a more stable product through a barrier of 114.9 kJ mol^{-1} (100.8 kJ mol^{-1} if ZPE correction is included), in agreement with experimental and theoretical values for Curtius rearrangements (95-115 kJ mol^{-1}).[8,24]

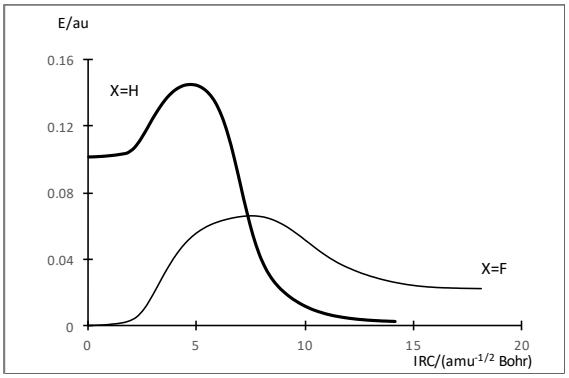

Figure 1. Molecular energy along the IRC.

Geometries and resonance forms for critical points

Table 1 shows the main geometrical parameters for the critical points in the path.

Table 1. Main geometrical parameters

Length/Angle	R	TS	P
O2-C1	1.202	1.208	1.167
N3-C1	1.417	1.301	1.210
H4-C1	1.097	1.151	1.986
N6-N5	1.123	1.098	1.095
H4-N3	2.057	1.761	1.008
N3-N5	1.250	1.770	
N3-C1-H4	109.1	91.6	23.9
C1-N3-N5	115.1	105.2	

Distances in Å and angles in degrees

The geometric parameters are in good agreement with the those obtained from both previous theoretical and experimental studies.[25-28] For the reagent, different bond distances are found for N5-N3 and N5-N6 bonds. The N5-N6 distance is closer to the

distance in N_2 while the N3-N5 length is larger. From these values it seems that the resonance form in Scheme I showing two double bonds, could not represent the structure of the molecule. It is confirmed when the values of the atomic charges for N5 and N6 are considered (-0.099 and 0.186 au respectively) as these values do not agree with the partial charges in the proposed resonance form. Moreover, DI values indicate that the resonance form with a single bond between N3 and N5 (DI=1.6 au) and a triple bond between N5 and N6 (DI=2.5 au) should contribute to describe the structure of the molecule.

In the transition state, BCPs indicate the H4 atom is bonded to C1 but it is not bonded to N3 yet. The DI values for H-C (0.7 au) and H-N (0.2 au) bonds agree with this interpretation. The C1-H4 bond is very close to that in the reagent (only 0.054 Å longer). The distance from H4 to N3 is also closer to that in the reagent than in the product, but in this case the difference is much larger (0.293 Å). The DI value for the C-H bond in the reagent (0.9 au) shows the covalent character of the bond, compared with the lower DI value for the H-N bond in the product (0.7 au), with a higher polarity. At this point the N5-N6 distance is similar to that in N_2 molecule in agreement with the value for the DI, 2.9 au.

For the product, the DI values for C-O and C-N are lower than 2 au. They are in better agreement with the slightly longer bond lengths (0.04-0.06 Å) than those corresponding to double bonds.

Electronic evolution of the reaction

Figure 2 shows the evolution of the main bonds involved in the reaction, C1-H4, N3-H4 and N3-N5, displaying their bond lengths and $\rho(\boldsymbol{r}_c)$ values. The C1-H4 distance increases along the reaction path showing the most important variations in the central part of the path, after the transition state. As expected, a BCP for the C1-H4 bond could be found at the beginning of the reaction, but it remains beyond the TS until IRC around 1.7 $amu^{-1/2}$ Bohr. At this point of the reaction (hereafter called point C) the "new" (N3-H4) and "old" (C1-H4) bonds are equal in length. After this point, the C1-H4 BCP disappears and is replaced by the N3-H4 one. The BCP for the N3-N5 bond remains along the whole path although $\rho(\boldsymbol{r}_c)$ is lower than 0.1 au after the transition state. Overall, the structure of the TS could be roughly described as "an isolation of N_2", whereas the most significant bond rearrangement takes place after the TS. From a formal point of view, three different phases could be distinguished in this one-step reaction: i) phase I, between the reagent and the TS; ii) phase II, between the TS and the point C; and iii) phase III, after the point C.

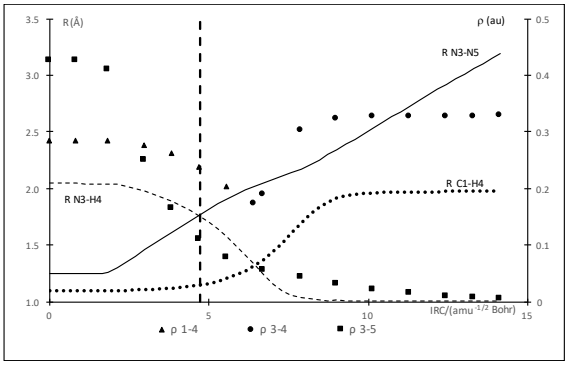

Figure 2. Variation of main bond lengths (lines) and the corresponding $\rho(\boldsymbol{r}_c)$ values (points). The dashed line indicates the position of the TS.

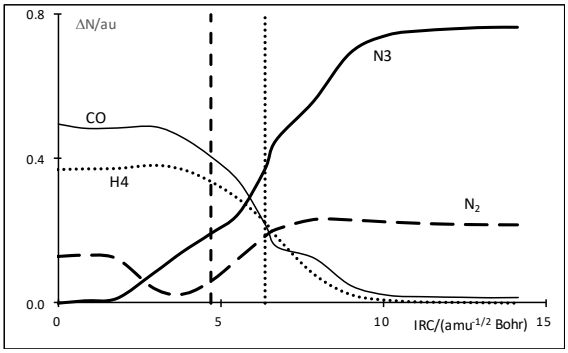

Figure 3. Evolution of electronic population for selected fragments. Dashed and dotted vertical lines indicate the position of TS and point C, respectively.

Figure 3 shows the evolution of electronic population for diverse fragments of the system along the reaction. We notice that N_2 fragment is still positively charged at the TS (the positive

partial charge on N6). It only becomes neutral at the end of the reaction. N3 gets more and more electron density as the reaction evolves, mainly taken from C2 and H4.

As previously observed in a long series of compounds[29-31] QTAIM charges do not support the resonance forms usually employed to describe azides and isocyanates. Thus, QTAIM charges for N5 and N6 in the azide are, respectively, -0.1 and +0.2 au in the azide, and that of N3 is -1.2 au in the isocyanate.

IQA analysis: electron density phases along the reaction

By applying expresion {1} to the H-migration process represented in scheme I we observe (Table 2) that: i) TS formation implies more repulsive interatomic coulombic interactions, not compensated by the variation of exchange-correlation interactions and atomic stabilizations; whereas ii) exchange-correlation interactions give rise to the exothermic character of the reaction.

Figure 4 shows E_{intra} for the six atoms of the molecule. We notice that N5 stabilizes continuously along the reaction, whereas C1 destabilizes. During phase I the variation of N5 exceeds significantly that of C1, and the opposite trend appears in phases II and III. Positive values of ΔE_{intra}(C1) correspond, as usual, with negative increments of electron population of C1 basin. In contrast, the electron population of N5 diminishes along phase I. In this case the negative ΔE_{intra}(N5) value can be explained as a consequence of the large increase of the volume due to the breakdown of the N3-N5 bond.

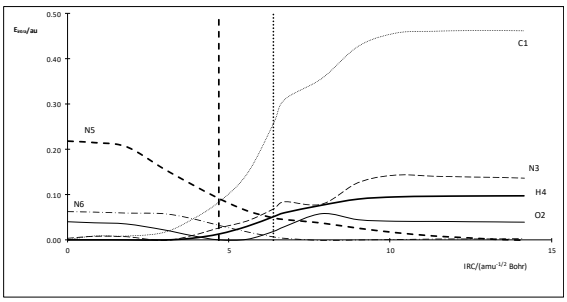

Figure 4. E_{intra} values along the IRC. Dashed and dotted vertical lines indicate the position of TS and point C, respectively.

Figure 5 shows the evolution of E_{inter} and their components, V_C and V_{XC}, during the reaction for the most significant bonds.

E_{inter} profile is basically ruled by four atomic pairs (Table 3): two of them stabilize along the reaction (C1-N3 and N3-H4) and other two destabilize (C1-H4 and N3-N5). Whereas C1-N3 displays a near similar behaviour in the 3 formal phases of the reaction, the variation of E_{inter} for the other three bonds are significant only in certain phases: N3-N5 in phase I and C1-H4 and N3-H4 in phases II and III. We also notice a significant stabilization of O2-C1 and destabilization of O2-N3 in phases II and III. Finally, we also observe that the components of ΔE_{inter}(N5,N6) nearly compensate in phase I.

Table 2. IQA decomposition of $\Delta E^{\neq}$ and ΔE values

	R→TS		R→P	
Component	X=H	X=F	X=H	X=F
ΔV_C	**0.2087**	**0.2627**	0.2323	0.1500
ΔV_{XC}	-0.0863	**0.2144**	**-0.7450**	0.3733
ΔE_{intra}	-0.0783	-0.4109	0.4145	**-0.5028**

All values in au

Table 2. IQA decomposition of $\Delta E^{\neq}$ and ΔE values

	R→TS		R→P	
Component	X=H	X=F	X=H	X=F
ΔV_C	**0.2087**	**0.2627**	0.2323	0.1500
ΔV_{XC}	-0.0863	**0.2144**	**-0.7450**	0.3733
ΔE_{intra}	-0.0783	-0.4109	0.4145	**-0.5028**

All values in au

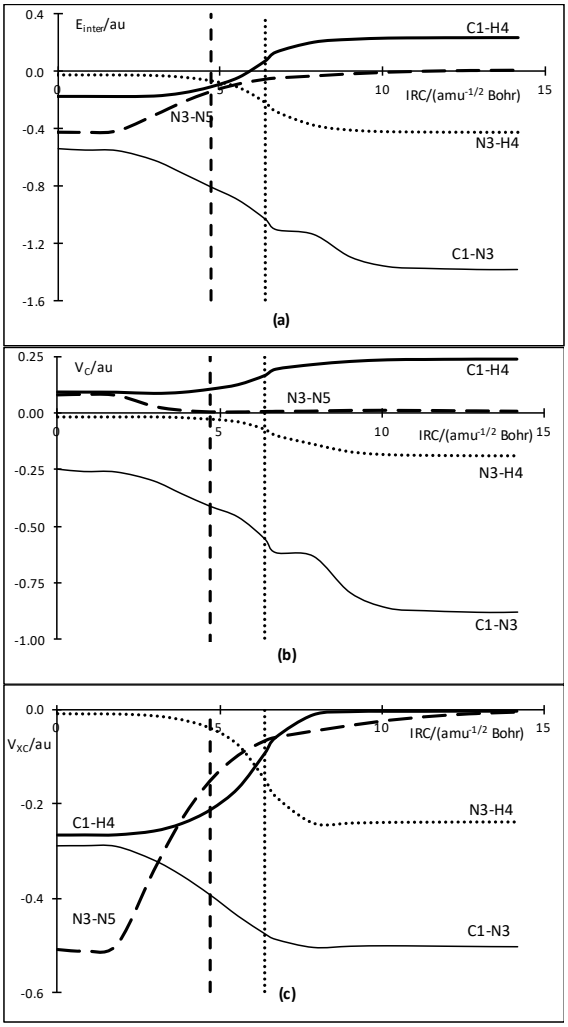

Figure 5. E_{inter} values and its components V_C and V_{XC} along the IRC. Dashed and dotted vertical lines indicate the position of TS and point C, respectively.

IQA analysis reveals that, for polar bonds, V_C leads most of the above detailed E_{inter} variations. ΔV_C is even significant for less polar bonds: N3-N5 along phase I (diminishing ΔE_{inter} by 27%) and C1-H4 in all phases (ΔV_C ranging from 18 to 45 % of ΔE_{inter}).

Table 3. Largest components of $\Delta E^{\neq}$ between TS and reactants

	R→TS		TS→P	
Component	X=H	X=F	X=H	X=F
ΔV_C(C1,O2)			**-0.2450**	0.0708
ΔV_{XC}(C1,N3)	**-0.1034**	-0.0885	**-0.1107**	-0.0996
ΔV_C(C1,N3)	**-0.1637**	-0.0216	**-0.4677**	-0.0048
ΔV_{XC}(C1,X4)			**0.2080**	**0.1476**
ΔV_C(C1,X4)	0.0124	**0.2925**	**0.1327**	**0.1509**
ΔV_C(O2,N3)			**0.1493**	0.0037
ΔV_{XC}(N3,X4)			**-0.1970**	**-0.2083**
ΔV_C(N3,X4)			**-0.1639**	0.0059
ΔV_{XC}(N3,N5)	**0.3570**	**0.4426**	**0.1454**	0.0585
ΔV_{XC}(N5,N6)	**-0.1075**	**-0.1256**		
ΔV_C(N5,N6)	**0.1092**	**0.1154**		
ΔV_{intra}(C1)	-0.0763	**-0.1200**	**0.3787**	**-0.1225**
ΔV_{intra}(N3)			**0.1089**	0. 0803
ΔV_{intra}(N5)	**-0.1273**	**-0.1825**		
All values in au				

We highlight that phase I is clearly different from the others. IQA values show that the destabilizing effect of breaking the N3-N5 bond is nearly completed during phase I. Moreover, breaking N3-N5 is the only significant process in this phase. Atomic electron populations indicate that a N_2 unit is nearly formed (with a positive partial charge at N6). Electron density moves from the N_2 frame to the N3 basin in this phase, whereas the reverse electronic displacement is observed in phases II and III. H4 migrates once phase I is finished. In contrasts, IQA analysis does not support to distinguish between phases II and III.

As a summary, the analysis of the geometries and the electron density along the reaction as well as the IQA analysis show that during phase I, between the reagent and the TS, the N_2 molecule goes away and only after that point during phases II and III, the C1-H4 bond begins to break and the new N3-H4 bond appears.

Substitution by Fluorine

In order to understand the changes when the TS of the reaction is displaced to the products, we substitute the migrating H atom by a F atom. In this case, as the energy profile reveals (Figure 1, for X=F), the product is less stable than the

reagent and the barrier, 174.3 kJ mol^{-1} (158.9 kJ mol^{-1} with ZPE correction), becomes higher than those usual for these rearrangements, because of the inclusion of a F atom. Moreover, comparing IRC curves, we observe that the TS is not so close to the reagent.

Table 4 shows the main geometrical parameters for the critical points in the path and Figure 6 shows the variations of the bond lengths and density values at the BCPs along the IRC.

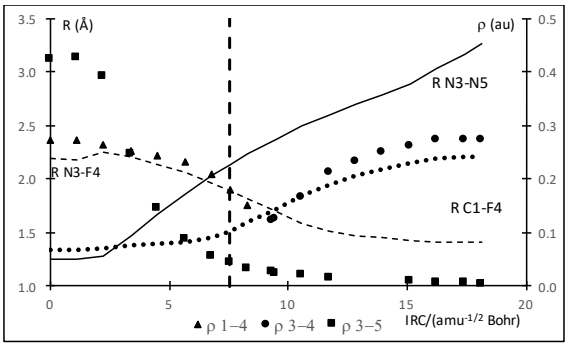

Figure 6. Variation of main bond lengths (lines) and the corresponding $\rho(\boldsymbol{r}_c)$ values (points) along the F migration. The dashed line indicates the position of the TS.

Table 4. Main geometrical parameters for the F-substituted molecule

Length/Angle	R	TS	P
O2-C1	1.187	1.170	1.156
N3-C1	1.396	1.304	1.247
F4-C1	1.338	1.518	2.206
N6-N5	1.122	1.095	1.095
F4-N3	2.199	1.889	1.413
N3-N5	1.250	2.140	
N3-C1-F4	107.1	83.7	36.5
C1-N3-N5	114.4	100.8	

Distances in Å and angles in degrees

The reagent and the product are very similar to those in the previous reaction. For the TS, the F atom is bonded to C1 but there is not a BCP connecting N3 to F yet. However, DIs for F-C (0.7 au) and F-N (0.7 au) bonds arise the same value at this point. The bonds C1-H4 and N3-H4 are closer to that in the reagent but the differences are bigger regarding to those found for the previous molecule. Also, the distance N3-N5 is larger than that found for the reaction with H. The point C, where the BCP for F-N appears, is achieved for IRC = 1.8 amu$^{-1/2}$ Bohr. Therefore, the three same formal phases could be considered for this reaction.

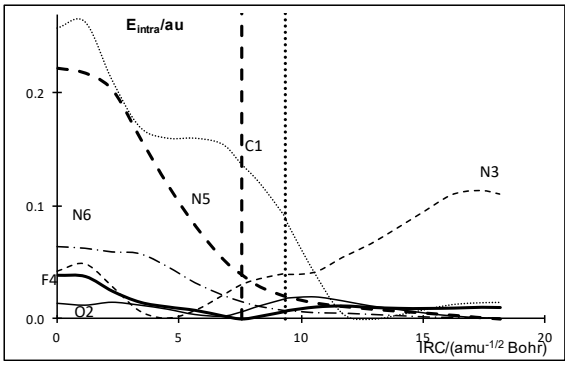

Figure 7. E_{intra} along the IRC for the F-substituted molecule. Dashed and dotted vertical lines indicate the position of TS and point C, respectively.

N_2 is again positive at the TS, but less than in the H migration. On the other hand, the electronegativity of F avoids the continuous increasing of electron population in N3 basin (supplementary material).

Table 2 shows that for the F-migration process, both the TS formation and the endothermic character are due to destabilization of electrostatic and exchange-correlation interactions, not compensated by atomic stabilizations.

Figure 7 exhibits the variation of the intratomic energies and it could be compared with Figure 4. Contrasting what was found for H migration, both N5 and C1 stabilize during the reaction. For C1 the stabilization is the result of the continuous increase of population and volume. For N5 the volume decreases continuously, whereas the population only decreases during phase I. The only atom with significant destabilization is N3, specially in phases II and III

when the volume significantly decreases. The continuous change in C1 along the three phases suggests that C1-F4 starts to break even at the same time the N_2 molecule goes away.

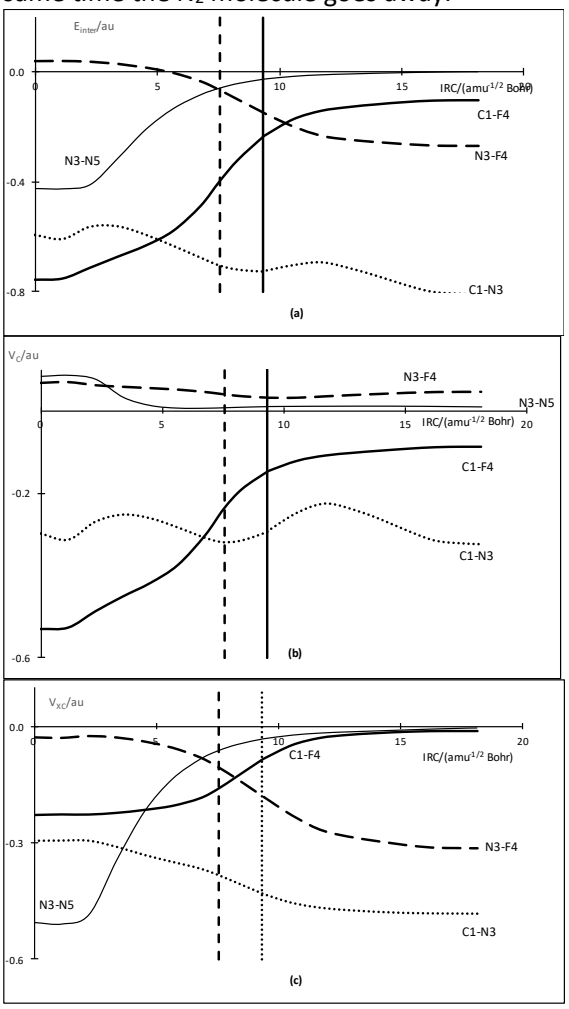

Figure 7. Variation of the E_{inter} energies (a) and its components V_C(b) and V_{XC}(c) for the bonds involved in the rearrangement for the F-substituted

In this case, E_{inter} profile cannot be reproduced on the basis of the four bonds exhibiting formal changes (Table 3). All V_C interactions are needed because of the amount of atomic charges introduced by F in the system. This is particularly true for formal phase II (data not shown). Nevertheless, the four bonds display again the largest ΔE_{inter} values. For these bonds, V_C contribution is less important than for the other reaction. E.g. ΔV_C represents only 20% of ΔE_{inter}(C1,N3) in phase I, compared to 61% in the same phase of H migration. This can be explained because in this case: i) in spite that absolute values of atomic charges are larger, their changes are much smaller; and ii) C1-N3 bond distance shortens less.

The most noticeable qualitative difference with H-migration is found in ΔE_{inter}(F4,C1) which is already high in phase I (both compared to the same phase for H-migration and to other phases for F-migration, see Figures 4 and 7). For the N3-N5 bond the changes in energy again happen before the TS. The variations after that point are even lower than those for the molecule with H. The bond C1-F4 begins to change before the TS (0.36 au compared to 0.07 au for C1-H4) mainly due to the electrostatic component: V_C varies 0.29 au before the TS for the C1-F4 bond and only 0.01 au for the C1-H4 bond. The interatomic energy between N3 and F4 varies 0.10 au before the TS and 0.20 au after it and it is mostly of electrostatic nature.

Therefore, this process seems to involve syncronous break of N3-N5 and C1-F4 bonds, and no phases should be distinguished according to IQA analysis.

Conclusions

Although the two Curtius rearrangements studied in this paper take place in one stage, two phases could be distinguished in one case. Thus, the migration of a hydrogen atom takes place in two consecutive phases: separation of N_2, and bond rearrangement (breakdown of the C-H bond, and formation of the new N-H bond). When the migration is undergone by a fluorine atom the process is really concerted and no electronic phases can be distinguished.

The TS for the H-migration studied in this work does not represent an intermediate state between reagent and product for the migration of the H atom, but for the isolation of the N_2 molecule. When the atom involved in the migration is fluorine, the migration happens before (closer to the TS) and so, the TS is more similar to the product.

The IQA analysis represents a very good tool to understand the changes along the reaction, revealing, in this case, different electron density evolutions for H and F migration and which are the energy components dominating at each part of energy profile. IQA analysis also indicates the scarce relevance (in terms of energy) of the point where BCPs appear or disappear.

Acknowledgments

We thank Xunta de Galicia for financial support through ED431C 2019/24.

Keywords: QTAIM, IQA approach, Curtius rearrangement, electron density analysis.

References and Notes

1. V.I. Minkin, *Pure & Applied Chemistry* **1999**, *71*, 1919-1981.
2. T. Curtius, *Berichte der deutschen chemischen Gesellschaft* **1890**, *23*, 3023-3033.
3. N. P. Gritsan, M. S. Platz, W. T. Borden, *Computational Methods in Photochemistry* **2005**, *13*, 235-356.
4. M. V. Zabalov, R. P. Tiger, *Russian Chemical Bulletin* **2012**, *61*, 1694-1704.
5. J. Liu, S. Mandel, C. M. Hadad, M. S. Platz, *Journal of Organic Chemistry* **2004**, *69*, 8583-8593.
6. M. V. Zabalov, R. P. Tiger, *Russian Chemical Bulletin* **2005**, *54*, 2270-2280.
7. M. V. Zabalov, R. P. Tiger, *Russian Chemical Bulletin* **2007**, *56*, 7-13.
8. V. Tarwade, O. Dmitrenko, R. D. Bach, J. M. Fox, *Journal of Organic Chemistry* **2008**, *73*, 8189-8197.
9. R. Kakkar, S. Zaidi, R. Grover, *International Journal of Quantum Chemistry* **2009**, *109*, 1058-1069.
10. R. W. F. Bader, Atoms in Molecules; University Press: Oxford, **1990**.
11. R. F. W. Bader, *Chemical Reviews* **1991**, *91*, 893-928.
12. A.M. Pendás, E. Francisco, M.A. Blanco, C. Gatti, *Chemical European Journal* **2007**, *13*, 9362-9371.
13. R.F.W. Bader, *Journal of Physical Chemistry A* **2009**, *113*, 10391-10396.
14. S.J. Grabowski, J.M. Ugalde, *Journal of Physical Chemistry A* **2010**, *114*, 7223-7229.
15. A.M. Pendás, J. Hernández-Trujillo, *Journal of Chemical Physics* **2012**, *137*, 134101-134102.
16. I. Cucrowski, J.H. de Lange, A.S. Adeyinka, P. Mangondo, **2015**, *1053*, 60-76.
17. A. Nouri, E. Zahedi, M. Ehsani, A. Nouri, E. Balali, *Computational and Theoretical chemistry*, **2018**, *1130*, 121-129.
18. M.A. Blanco, A.M. Pendás, E. Francisco, *Journal of Chemical Theory and Computation* **2005**, *1*, 1096-1109.
19. E. Francisco, A.M. Pendás, M.A. Blanco, *Journal of Chemical Theory and Computation* **2006**, *2*, 90-102.
20. G. W. T. M. J. Frisch, H. B. Schlegel, G. E. Scuseria, M. A. Robb, J. R. Cheeseman, G. Scalmani, V. Barone, B. Mennucci, G. A. Petersson, H. Nakatsuji, M. Caricato, X. Li, H. P. Hratchian, A. F. Izmaylov, J. Bloino, G. Zheng, J. L. Sonnenberg, M. Hada, M. Ehara, K. Toyota, R. Fukuda, J. Hasegawa, M. Ishida, T. Nakajima, Y. Honda, O. Kitao, H. Nakai, T. Vreven, J. A. Montgomery, Jr., J. E. Peralta, F. Ogliaro, M. Bearpark, J. J. Heyd, E. Brothers, K. N. Kudin, V. N. Staroverov, R. Kobayashi, J. Normand, K. Raghavachari, A. Rendell, J. C. Burant, S. S. Iyengar, J. Tomasi, M. Cossi, N. Rega, J. M. Millam, M. Klene, J. E. Knox, J. B. Cross, V. Bakken, C. Adamo, J. Jaramillo, R. Gomperts, R. E. Stratmann, O. Yazyev, A. J. Austin, R. Cammi, C. Pomelli, J. W. Ochterski, R. L. Martin, K. Morokuma, V. G. Zakrzewski, G. A. Voth, P. Salvador, J. J. Dannenberg, S. Dapprich, A. D. Daniels, Ö. Farkas, J. B.

Foresman, J. V. Ortiz, J. Cioslowski, and D. J. Fox, Gaussian, Inc., Wallingford CT, 2009.
21. AIMAll (Version 17.11.14), Todd A. Keith, TK Gristmill Software, Overland Park KS, USA, 2017 (aim.tkgristmill.com)
22. R. W. F. Bader and M.E. Stephens, *J. Am. Chem. Soc.* **1975**, *97*, 7391-7399.
23. X.Fradera, J. Poater, S. Simon, M. Duran and M. Sola, *Theor Chem Acc* **2002**, *108*, 214-224.
24. C. Wentrup, H. Bornemann, *European Journal of Organic Chemistry* **2005**, 4521-4524.
25. K. Yokoyama, S. Takane, T. Fueno, *Bulletin of the Chemical Society of Japan* **1991**, *64*, 2230-2235.
26. A. M. Mebel, A. Luna, M. C. Lin, K. Morokuma, *Journal of Chemical Physics* **1996**, *105*, 6439-6454.
27. W. A. Shapley, G. B. Bacskay, *Journal of Physical Chemistry A* **1999**, *103*, 6624-6631.
28. A. L. L. East, W. D. Allen, *Journal of Chemical Physics* **1993**, *99*, 4638-4650.
29. R. Glaser and G. S. C. Choy, *Journal of the American Chemical Society*, **1995**, 115, 2340.
30. J. L. Lopez, A. M. Graña and R. A. Mosquera, *Journal of Physical Chemistry A* **2009**, *113*, 2652-2657.
31. M.J. González-Moa and R. A. Mosquera, *Journal of Physical Chemistry* A **2005**, 109, 3682.

Additional Supporting Information may be found in the online version of this article.